Direct Measurement of Elbow Joint Angle Using Galvanic Couple System

Xi Mei Chen, Shovan Barma, *Member, IEEE*, Sio Hang Pun, *Member, IEEE*, Mang I Vai, *Senior Member, IEEE*, and Peng Un Mak, *Senior Member, IEEE*

***Abstract*— This paper proposes a simple approach to measure the elbow joint angle (EJA) using galvanic coupling system (GCS), directly; whereas, the traditional methods involved in either complex machine-learning task or arm movement models in which the consideration of model parameters are not accurate very often. First, a correlation between the EJA and GCS data has been established by defining a polynomial function based on a simple six-impedance model of human upper arm, where the EJA (θ) has been achieved by moving the forearm along the sagittal and transverse planes with different loads (empty hand, 1 and 2 kg). The coefficients of the polynomial are estimated based on the polynomial fit technique in which the actual angles (reference frame) are calculated by using motion data. In total, eleven subjects (seven males and four females) with the age of 30 ± 6 years have been considered during the experiment. However, the GCS data of eight subjects are used to derive the correlation, exclusively. Furthermore, the influence of muscle fatigue and different loads on the derived correlation has been studied. Next, based on the derived correlation, the EJA has been measured in two parts—inside and outside tests by considering six subjects. The results show that the proposed idea can measure the EJA very effectively with error up to ±0.11 rad (6°). Moreover, in a performance comparison, the proposed approach shows its compatibility by indicating low complexity, higher accuracy, and easy to measure.**

***Index Terms*— Forearm movement, galvanic coupling system (GCS), measurement of elbow joint angle (EJA), upper arm muscle.**

Manuscript received May 4, 2016; revised September 17, 2016; accepted October 26, 2016. Date of publication February 8, 2017; date of current version March 8, 2017. This work was supported in part by the Science and Technology Development Fund of Macau under Grant 063/2009/A, Grant 024/2009/A1, Grant 087/2012/A3, Grant 047/2013/A2, and Grant 093/2015/A3 and in part by the Research Committee of the University of Macau under Grant MYRG2014-00010-AMSV, Grant MYRG079(Y1-L2)-FST12-VMI, and Grant MYRG103(Y1-L3)-FST13-VMI. The Associate Editor coordinating the review process was Dr. Wendy Van Moer.

X. M. Chen and M. I Vai are with the State Key Laboratory of Analog and Mixed-Signal VLSI, University of Macau, Macau 999078, China, and also with the Department of Electrical and Computer Engineering, Faculty of Science and Technology, University of Macau, Macau 999078, China (e-mail: sammy.cxm@gmail.com; fstmiv@umac.mo).

S. Barma is with the Department of Electronics and Communication Engineering, Indian Institute of Information Technology, Guwahati 781001, India (e-mail: shovan@iiitg.ac.in).

S. H. Pun is with the State Key Laboratory of Analog and Mixed-Signal VLSI, University of Macau, Macau 999078, China (e-mail: lodgepun@umac.mo).

P. U. Mak is with the Department of Electrical and Computer Engineering, Faculty of Science and Technology, University of Macau, Macau 999078, China (e-mail: fstpum@umac.mo).

Color versions of one or more of the figures in this paper are available online at http://ieeexplore.ieee.org.

Digital Object Identifier 10.1109/TIM.2017.2654138

I. Introduction

THE measurement of elbow joint angle (EJA) during multidegree arm movement which takes place in our various daily life activities is very important, especially to assist physically disabled, injured or elderly people for self-rehabilitation purpose or designing upper-limb power-assist exoskeletons robot [1]–[3]. In recent, there are several attempts have been made to measure the EJA based on mechnanomyogram and electromyography (EMG) [2], [4]–[9]. Most of the works of EJA measurement follow mainly two particular approaches; such as either model based or machine learning (ML) or both. The ML-based approaches include acquisition of different physiological signals at certain states or positions of arm's movement, and then define features followed by classification using numerous kinds of ML techniques such as artificial neural network (ANN) [10], fuzzy logic [11], support vector machine [12], time-delayed ANN [13], and so on. However, these methods involve in very complex ML mechanism, and the overall performance of the systems always depends on feature selection and training data set. In contrast, the model-based approaches measure the EJA by considering different models of human arm's motions/movements [14]–[16]. The performances of such approaches completely depend on consideration of the model and its chosen model parameters. Eventually, selection of accurate model parameters is very difficult as any human activity comprises of several factors, which further affects the measured results. On the other hand, there are some other kinds of approaches which only focus on specific signal processing mechanisms, including different time-frequency methods on physiological signal of hand motions, which are acquired by different sensors [17], [18]. Nevertheless, the methods are simple, but the results are pragmatic and lack proper theoretical foundation concerned with different arm movements. Furthermore, most of works are performed without clearly addressing the influence of muscle fatigue factor, which is very relevant during any muscular activity measurement [19]–[21]. Therefore, a direct approach is very essential to measure the EJA which should be very simple with proper theoretical basis and less interfered by muscle fatigue and loads on hand.

Certainly, the human upper arm consists of five major muscles (biceps, triceps, brachioradialis, extensor carpi radialis longus, and deltoid) which conjointly enable the forearm either to rotate or to strengthen or both. Several studies reported that there is a significant variation of muscle

length and physiological cross-sectional area (PCSA) of upper arm muscles during change of EJA [7], [9]–[12], [22]–[25]. Eventually, our previous work confirms that there is a significant influence of limb gestures (e.g., change of EJA) on the human body communication by displaying the profound variations on channel gain/attenuation [26]. Such evidence fascinates us to investigate the correlation between the EJA and upper arm muscles, which can be employed to estimate the EJA directly by measuring the gain/attenuation only. Nonetheless, such method appears very simple compared to earlier machine-learning or model-based approaches.

In this connection, the human muscles act as electrical transmission lines which can be represented by the parameters including resistance (R), reactance (X), and phase angle (φ) [27], [28]. The aforementioned geometrical variations (length and PCSA) of the upper arm muscles during change of EJA also affect the variation on R, X, and φ, and such changes can be measured by the galvanic coupling system (GCS) [27], [29]. It is a noninvasive, easily repeatable, low cost, and quantitative measurement technique and also can be employed on human subjects [30]. Basically, in GCS, an alternating electrical signal is applied by two transmitting electrodes and received by two detecting electrodes simultaneously which further guides to measure R, X, and φ. However, the measured values depend on various factors, including applied input signal, geometric parameters of the muscle (e.g., changes in muscle shape or volume), tissue parameters (e.g., dielectric properties of the tissue, fat level, water level), and placement of the electrodes [31]. Nonetheless, the mentioned factors of the tissue pathology in human subject are not possible to estimate directly, but there are several studies which have been performed including placement of electrodes, characteristics of the applied input signal [32]–[34].

In this view, this paper proposes a simple method to measure the EJA using GCS. First, a correlation between the EJA and change of muscle impedances is derived by polynomial function. Then, the values of the coefficients of the polynomial are devised using polynomial fitting technique where the actual angle is estimated by a camera. In this regard, EJA has been achieved by moving the forearm along sagittal and transverse planes with different loads (empty hand, 1 and 2 kg) in hand. Next, based on the devised correlation, the EJA has been measured. In addition, influence of different factors including muscle fatigue on the devised correlation has been studied. In total, eleven subjects have been participated in these experiments. Exclusively, acquired data of eight subjects are considered to establish the correlation. Then, the EJA has been measured considering six subjects in two parts—inside (three out of eight subjects) and outside tests (rest three subjects). Further, the performance of the proposed idea has been compared with the existing methods. The results show that the proposed idea is very simple and much effective to estimate the EJA.

The rest of this paper is organized as follows. Section II describes the methodology followed by experiments in Section III. Section IV explains the results and discussion, and the conclusions are drawn in Section V.

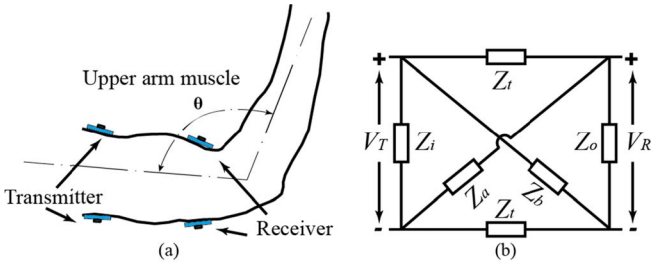

Fig. 1. (a) Schematic of the galvanic couple system on upper arm muscles. (b) Equivalent circuit model of upper arm.

II. Methodology

To investigate the correlations between the EJA and electrical properties (impedance) of the upper arm muscles, a GCS which includes pairs of electrodes (transmitter and receiver) has been used as shown in Fig. 1(a). Certainly, all the five muscles are considered as a group of muscles, which can be represented by a six impedance equivalent electrical circuit model as shown in Fig. 1(b) [27], [30]. The equivalent circuit includes input and output terminals, and six impedances including input impedances (Z_i), output impedances (Z_o), transverse impedance (Z_t), and two butterfly cross impedances (Z_a and Z_b). An alternating signal (V_T) is applied through input terminal and the corresponding signal is acquired (V_R) by the output terminal. Due to impedance of muscles, the received signal attenuates significantly with respect to the triggered input signal, which can be defined by a transfer function (1), where A is the attenuation in dB, $H_A = V_R/V_T$, and K is the correcting factor which depends on the modeling methods, parameters to be determined, and measurement precisions [27]. The values of H_A is dependent on the six impedances. During the change of EJA, the impedances change accordingly as mentioned before, i.e., H_A and so A. Therefore, how the impedances are varying with EJA changes could lead to the estimation of EJA by directly acquiring A using GCS

$$A = 20 \log_{10} H_A + K. \tag{1}$$

The simulation technique of signal transmission paths on human muscles using GCS based on six impedance model has been detailed in [27]. Following their work, the Z_i and Z_o can be estimated by (2), based on cylindrical model of human limb which includes five layers (skin, fat, muscle, bone, and bone marrow):

$$Z_i = Z_o = \sum_{l=1}^{5} \frac{T_l}{\sigma_{lf} \pi r^2 + j\omega \varepsilon_{rlf} \varepsilon_0 \pi r^2} \tag{2}$$

where l refers to specific layer, T_l refers to the thickness of the different layers (skin, fat, muscle, bone, and bone marrow), r, σ_{lf}, ε_0, and ε_{lf} refer to radius, conductivity, free space permittivity, and relative permittivity of the corresponding layers respectively; ω is the applied angular frequency. Following the work in [27], the two butterfly impedances can be transferred into sum of transverse impedances with input

and output impedances; $Z_a = Z_i + Z_t$ and $Z_b = Z_o + Z_t$. The Z_i and Z_o are constant for a specific group of muscles (here upper arm muscles) but the value of the transverse impedance Z_t changes due to change of EJA as its value is dependent on the geometrical parameters (length and PCSA) of the upper arm. In the literature, the human muscles can be represented by the electrical model including resistive (R) and capacitive (C) part connected in parallel [27], [28]. Thus, Z_t can be defined by

$$Z_t = \frac{1}{\sum_{l=1}^{5}\left(\frac{1}{R_l} + j\omega C_l\right)} \tag{3}$$

where R_l and C_l are the resistance and capacitance of the lth layer according to the electrical model of human muscles. Further, considering the other parameters, such as muscle transmitting length (L), cross-sectional area of each layer (S_l), tissue dielectric properties (σ_{lf} and ε_{rlf}), the Z_t can be rewritten as (4)

$$Z_t = \frac{L}{\sum_{l=1}^{5}\sigma_{lf}S_l + j\omega\varepsilon_0\sum_{l=1}^{5}\varepsilon_{rlf}S_l}. \tag{4}$$

Meanwhile, during electrical signal transmission through muscles, the resistive part becomes more dominant than capacitive part for certain frequencies [28]. For, example, considering (3) and (4), the $1/R = \Sigma(1/R_l)$ and $C = \Sigma C_l$ can be calculated; assuming, muscle transmitting length (MTL), $L = 10$ cm (interelectrode distance), PCSA = 50 cm^2; it can be seen that $X_c \gg R$; where all values of σ_{lf} and ε_{lf} for different layers are at 20 kHz [35]. Therefore, resistance, R is more significant than C. Now, as per general physics, the resistance of the upper arm muscle can be referred as

$$Z_t \approx R\,\alpha\frac{MTL}{PCSA}. \tag{5}$$

As aforementioned, during the change of EJA (θ) the *MTL* and *PCSA* change very significantly; for instance, during elbow flexion to extension position the upper arm muscles expanses (i.e., *MTL* increases) but overall *PCSA* decreases. In contrast, *MTL* and *PCSA* decreases and increases respectively during elbow extension to flexion position. All though, both of the cases make changes of R (i.e., Z_t) in same way (increase or decrease). Such phenomenon leads to change on received signal, V_R (i.e., A), which can be measured by (1) for known V_T. However, it is very difficult to measure the *PCSA* during change of EJA as the structures of all muscles are not similar, even more, a single muscle is not uniform at everywhere; even more, *PCSA* varies person to person. Besides, *MTL* depends not only on the placement of the electrodes but also it is influenced by regions beyond that. Therefore, change of Z_t can be measured considering, $\eta = MTL/PCSA$, rather than *MTL* and *PCSA* individually as the effects on their variations toward the change of Z_t are similar.

As per literature, several works noted that the muscle length changes proportionally, especially biceps, during the change of the EJA, but not linearly. In this connection, a relation between the EJA with upper arm muscle momentum and muscle length using polynomial fitting technique has been presented in [37]. As change of muscle length has direct impact on R, following their method and considering (4), (5), the transverse impedances can be written as polynomial function:

$$Z_t(\theta) = \eta(b_0 + b_1\theta + b_2\theta^2 + \cdots + b_k\theta^k) \tag{6}$$

where $b_0, b_1, b_2, \ldots, b_k$ are polynomial coefficients. Indeed, such changes of Z_t, replicate on V_R as well. Therefore, the attenuation can be transferred into a function of EJA and can be defined by

$$A(\theta) = \eta(b_0 + b_1\theta + b_2\theta^2 + \cdots + b_k\theta^k). \tag{7}$$

Next, the order of the polynomial and values of the coefficients can be determined by polynomial fit techniques using a reference frame. The value of the η is not the same across the upper arm region and it varies person to person; therefore, it is appropriate to consider value η by measuring length of the upper arm and *PCSA* across biceps muscle as it changes significantly during EJA changes. Hence, a correlation between the EJA and acquired signal can be established. Then, based on the derived correlation and acquiring the attenuation signal by employing GCS, the EJA can be estimated. In this regard, the characteristic of the acquired GCS signal (i.e., received signal) relies on the operating frequency of the triggering signal and placement of the electrodes. To achieve good response of GCS signal (i.e., high signal amplitude), the suitable operating frequency is 20–30 kHz (20 kHz in our experiment) with placement of electrodes pair circular symmetrically (i.e., on biceps and triceps) [26], [32]–[34], [36]. Besides, the longitudinal distance between the transmitter and receiver electrode pairs must encompass most of the upper arm muscles, especially biceps muscle (10 cm in our experiment).

TABLE I
DETAILS OF THE SUBJECTS

Sub[$]	Age (Yr)	$H^{\dagger}$ (cm)	$W^{\#}$ (kg)	Upper arm dimension		BMI
				$l^{\dagger}$ (cm)	$PCSA^{\ddagger}$ (cm^2)	
S1	26	172	52	26.6	39.0	19.0
S2[*]	27	184	60	20.5	44.1	19.5
S3[*]	26	166	50	18.6	52.7	19.8
S4	33	151	43	17.7	54.0	20.0
S5	35	165	54	25.2	62.1	20.4
S6	23	170	64	13.6	58.0	20.6
S7[*]	25	158	63	18.6	83.2	24.0
S8	28	186	90	31.3	86.5	25.3
S9	27	165	63	24.2	65.0	32.1
S10	32	158	61	24.8	75.8	24.4
S11[*]	24	163	58	22.6	76.9	21.8

[$]Subjects; [*]female subjects; [†]height; [#]weight; [†]length of the upper arm; [‡]physiological cross sectional area of across biceps muscle.

III. EXPERIMENT

A. Experimental Protocols

1) Subjects: In total eleven subjects (four females and seven males) with age of 30± 6 years have been considered during the experiment. All the subjects do not have any muscular disorder while the experiments have been performed. All of them have been informed about the assessment protocols and they

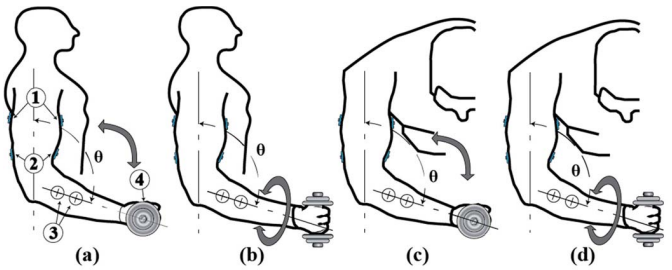

Fig. 2. Definition of EJA and different positions of the forearm movements for GCS data acquisition. (a) Forearm movement along the sagittal plane. (b) Supination and pronation with loads at certain angle along the sagittal plane. (c) Forearm movement along the transverse plane. (d) Supination and pronation with loads at a certain angle along the transverse plane.

have given their written consent. The concerned parameters of the subjects as indicated by "S" and associated numbers are listed in Table I which includes age, sex, height, weight, dimension of the right upper arm, and Body Mass Index from the second column consecutively. Besides, the length and PCSA across biceps muscle at normal [31]–[33] condition of the upper arm are also specified separately. During experiment, the eight subjects (S1–S8) are chosen to estimate the coefficients b_k ($k = 0, 1, 2, \ldots, k$) of the polynomial function (7). Finally, considering six subjects, the EJA has been estimated based on the derived polynomial function by conducting two kinds of test—inside (three subjects from S1–S8) and outside tests (S9–S11).

2) Hand Movements: Each subject has been asked to perform the right-hand movements having sitting position. During the hand movements, the upper arm has been kept in fixed position, while change of the EJA has been achieved by moving the forearm with empty hand and different loads (1 and 2 kg) as displayed in Fig. 2. The forearm movements are directed in three ways: 1) change of EJA along the parasagittal plane, while the upper arm is positioned downward vertically [Fig. 2(a)]; 2) change of EJA along the transverse plane with positing the right upper arm horizontally [Fig. 2(c)]; and 3) for both of the cases, the forearm is supinated and pronated with a certain angle (60° and 90°) as indicated in Fig. 2(b) and (d). Certainly, small marks are placed on the side of lower arm for trajectory tracking by camera. Before collecting the data, the subjects are told to practice elbow joint contraction and extension along the sagittal and transverse planes about one minute. Next, data are acquired by changing EJA in empty-handed. In the similar manner, the second and third sets of data have been acquired with 1 and 2 kg load on hand respectively. The subjects are given rest about 5 min after each of the performance.

B. Experimental Setup

An overall system overview of the experimental setup has been displayed in Fig. 3, which includes three main sections called GCS data, motion data, and data processing unit. However, an EMG data unit has been considered to monitor

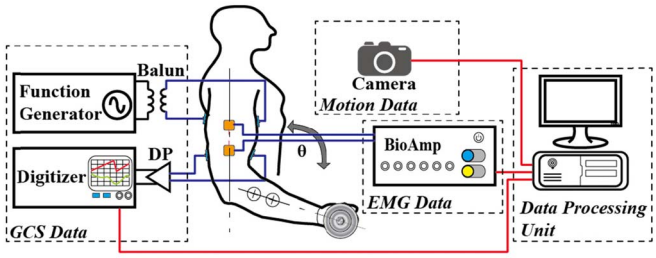

Fig. 3. System overview of the experimental setup.

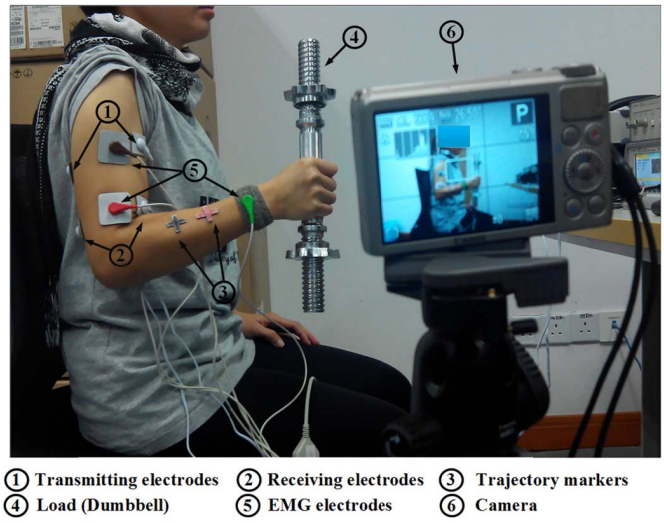

Fig. 4. Real life experimental setup for the GCS, camera, and EMG data acquisition during forearm movement along the parasagittal plane.

the fatigue of the upper arm muscles simultaneously during EJA changing. The GCS data unit consists of function generator and digitizer as displayed in Fig. 3. The triggering signals are provided by the function generator, which is connected to the human body via balun (low frequency) for safety reasons. In addition, the received signals are acquired from human body via a differential probe (DP). During change of EJA along either sagittal or transverse plane, there are significant variations on GCS data. In this connection, concurrently, another two sets of data—motion and EMG—are also acquired by camera and BioAmp (AD Instrument, PowerLab 15T), respectively. The motion data lead to calculate the actual angle of EJA, whereas the EMG data help to evaluate the muscle fatigue. Finally, all the three kinds of data are analyzed by data processing unit (Computer) which is comprised of different software packages, such as MATLAB for GCS and EMG data processing and TRACKER for video data processing.

A real-life experimental setup for data acquisition is displayed in Fig. 4, by indicated different components including camera, position of the electrodes of the galvanic coupling and surface EMG systems, trajectory markers, and load. The subjects are sitting normally and make the change of EJA as mentioned before. The camera captures the system movements aiming to estimate the actual EJA based on trajectory markers as depicted in Fig. 4 (see also Figs. 2 and 3). The EMG setup is used to measure the fatigue of the upper arm muscles to

TABLE II
ENVIRONMENT OF GCS DATA ACQUISITION SYSTEM

Parameters	Values
Triggering signal	Sinusoidal, 0.6 V, 20 kHz
Induced current	1.5±0.2 mA
Transmitting power	0 dBm
Inter-electrode distance	10 cm
Channel attenuation	25±3 dB
Received signal	0.03±0.01 V
System noise	-75±5 dBm
System SNR	45±5 dB

study its influence on EJA measurement. As the input signal frequency (20 kHz) of the GCS is much higher than the bandwidth (2–500 Hz) of the surface EMG, it does not affect the EMG data [37]. The GCS data acquisition and motion data acquisition have been detailed as follows.

Data Acquisition: A sinusoidal signal generated by a function generator (Agilent, 33250 A) with 0 dBm power has been applied to the human upper limb by a pair of stimulating electrodes of 20 × 20 mm^2 (Shenzhen Jurongda Science and Technology Ltd.). The receiving electrodes are placed about 6 cm away from the elbow joint and laterally oriented on the upper arm, whereas, the transmitting electrodes are place 10 cm apart from the receiving electrodes as shown in Fig. 4. The frequency of the triggering signal has been kept 20 kHz [29], [32]–[34]. The received signals are acquired by a DP (Agilent, 1141A) and simultaneously recorded by a digitizer (National Instrument, PXIe-5122) through a software interface with sampling frequency 200 kHz. However, the EMG data has been collected using BioAmp. Notably, the choices of type of electrodes for GCS and EMG data acquisition are Carbon and Ag/AgCl respectively. Such difference is due to the fact that the GCS system compromises of triggering input signal into human body and the carbon electrodes are preferable in such situations [38]. In summary, the overall environment of GCS data acquisition system has been displayed in Table II, which includes the characteristics of the triggering and receiving signals, system noise level and system Signal-to-noise ratio (SNR).

1) Motion Data Acquisition: The motion data are captured during EJA changes by a camera (Canon, Power Shot: S100), with frame rate of 42 ms/frame and sampling frequency 24 Hz which further uses as reference frame (actual angle). It captures the distinct markers which are placed on the forearm of the subjects as indicated in Fig. 4 (see also Fig. 2). Based on the relative positions of the markers, the actual EJA is calculated through the recording period. Certainly, the change of the EJA has been achieved by moving the forearm only while the upper arm always has been kept in fixed position along sagittal and transverse planes. The actual EJA angle has been evaluated by motion data analysis software (TRACKER), which tracks the trajectory of the markers and computes the angle with respect to reference line (fixed upper arm) (see Fig. 2).

2) Data Processing:

$$x_{\text{norm}}(t) = \frac{x(t)}{\max\{x(t)\}}. \tag{8}$$

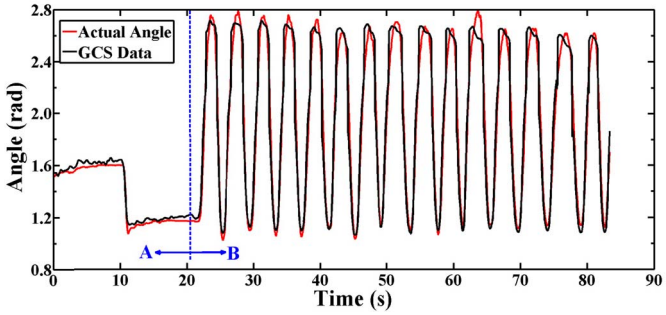

Fig. 5. Curve fitting between actual EJA and GCS data.

In these experiments, three kinds of data are collected—GCS, video and EMG data. The GCS data are affected by noise and incorporated with the artifacts. Therefore, the recorded raw GCS data are filtered by bandpass filtering between 15 and 25 kHz to reduce the noise and movement artifacts. Next, the envelopes of the GCS data are extracted by using the Hilbert transform. During GCS data processing, attenuation has been calculated simultaneously according to (1) and normalized by (8); where $x_{\text{norm}}(t)$ and $x(t)$ are the normalized and actual GCS envelopes. Certainly, the K is the correcting factor which is calculated as errors among different subjects in our work. A synchronization technique has been employed as the sampling frequencies of the GCS data and camera are not the same, which matches the time indices between the GCS data and calculated actual angle accurately. After that, the polynomial fitting technique is employed to find the correlation between the GCS data and EJA. On the other hand, EMG data are acquired separately to estimate the muscle fatigue [39], [40]. The data processing has been conducted by MATLAB.

IV. RESULTS AND DISCUSSIONS

A. Correlation Between Attenuation and EJA

1) Polynomial Fitting: The polynomial fitting technique has been adopted to find the values of the coefficients of the polynomial (7) which has been illustrated by considering a single subject in Fig. 5 in which the horizontal and vertical lines are refer to time (s) and angle (rad), respectively. First, the GCS data (black) are fit with the actual EJA movement (red) which has been calculated by the video data. Certainly, the attenuation of the GCS signal from any the part of human body influenced by the static or dynamic conditions of that part [36]. Therefore, to accomplish the reliable values of the coefficients of the polynomial (7), the GCS data have been acquired not only during the forearm is moving back and forth (see Fig. 2) but also in static; although the polynomial function refers to the direct correlation between the EJA angle and GCS data. To do so, the forearm has been kept unmoved at two certain angles of 1.0 and 1.6 rad at about 10 s each (i.e., total 20 s). After that, the forearm is being moved with angular velocity of 0.79 rad/s. The two steps has been depicted by A and B regions in Fig. 5, which last about 0–20 and 20–85 s, where the regions A and B denote the unmoved and moving conditions of the forearm respectively.

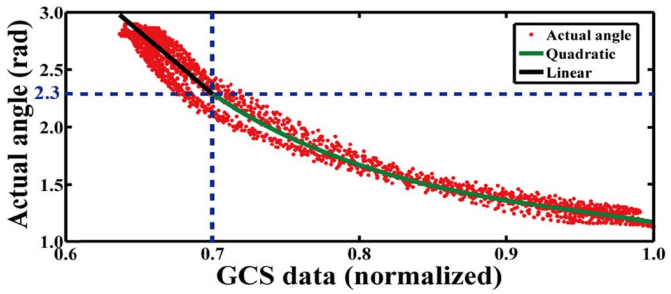

Fig. 6. Analysis of the curve fitting between GCS data and EJA.

As observed, the fitting is smoother in region "A" compared to the end part of region B. However, such variations are very small, which occur during anthropometric measurement.

The mean ± SD value of the root-mean-square error (RMSE) and correlation factor between the fit curve and the actual EJA curve is about 0.12 ± 0.08 rad and 0.94 ± 0.03, respectively, which is significantly small with respect to full EJA movement of 2.2 rad (130°) and the correlation value is considerably high. Therefore, the fit curve is very consistent.

Now, to determine the values of the coefficients in (7), first, the order of the polynomial is estimated empirically as $k = 2$. Now, the correlation is as

$$A(\theta) = \eta(b_0 + b_1\theta + b_2\theta^2). \tag{9}$$

In this regard, the fit curve of GCS data and actual EJA has been depicted in Fig. 6, in which the horizontal and vertical axes refer to normalized GCS data and the actual angle. As seen, along vertical axis, at higher ranges the EJA changes linearly, but at lower ranges it behaves like a curve. Based on visual inspection, the primary break point has been estimated which is between 2.0–2.5 rad. Next, aiming to find the optimum break point in this region, the mean-square error (MSE) has been calculated between the measured data and fitting line. The best fit has been achieved with break point at 2.3 rad with minimum MSE of 0.07 rad (about 3% of the full EJA movement), which is trivial in case of EJA estimation. In Fig. 6, the break point has been indicated by dotted lines. Therefore, the curve has been divided into two parts for $\theta \geq 2.3$ and $\theta < 2.3$ rad, and the corresponding equations are (10). The values of the coefficients are: $b_0 = 7.2$ and $b_1 = -6.2$ for $\theta \geq 2.3$ and $b_0 = 21.6$, $b_1 = -39.9$, and $b_2 = 19$ for $\theta < 2.3$. From (10), it is observed that the bio-impedance changes linearly with EJA for $\theta \geq 2.3$, but it changes in quadratic nature for $\theta < 2.3$. The linear and quadratic regions are depicted by black and green color, respectively, in Fig. 6

$$A = \begin{cases} b_0 + b_1\theta & \text{for } \theta \geq 2.3 \text{ rad} \\ b_0 + b_1\theta + b_2\theta^2 & \text{for } \theta < 2.3 \text{ rad.} \end{cases} \tag{10}$$

Finally, the values of the coefficients of eight subjects are: $b_0 = 7.2 \pm 1.1$ and $b_1 = -6.2 \pm 1.5$ for $\theta \geq 2.3$ and $b_0 = 21.6 \pm 8.0$, $b_1 = -39.9 \pm 17.2$, and $b_2 = 19.0 \pm 9.2$ for $\theta < 2.3$. Although the experiments and the simulation have been performed with careful considerations, such variations appear because of the simplification of the mathematical formulation, muscular parameters, and errors in anthropometric measurements.

TABLE III
IMPACT OF LOADS IN HAND ON POLYNOMIAL COEFFICIENTS

Loads	$\theta \geq 2.3$ (linear)		$\theta < 2.3$(quadratic)		
	b_0	b_1	b_0	b_1	b_2
Empty	6.5±1.9	-5.0±2.3	21.4±9.1	-39.6±20.6	19.0±11.3
1 kg	7.2±0.6	-6.3±1.0	19.1±6.5	-34.1±14.2	15.6±8.2
2 kg	7.9±1.0	-7.3±1.4	24.3±8.5	-46.1±16.8	22.4±8.3
Overall	**7.2±1.1**	**-6.2±1.5**	**21.6±8.0**	**-39.9±17.2**	**19.0±9.2**

Furthermore, the impact of supination and pronation of the forearm has been studied which occurs very often during EJA changes with or without load. Therefore, maintaining a certain angle 1.0 rad (60°) and 1.6 rad (90°), the forearm is supinated and pronated for both of the cases of the hand movements (along sagittal and transverse planes). The measured attenuation varies ±4%; i.e., such supinated and pronated of the forearm has negligible effect on the change of received signal. Therefore, such twisting has no effect on the change of muscle impedances of the upper arm.

2) Influence of Load: Further, the impact of the load (dumbbell weight) on the values of the polynomial coefficients (10) during different load condition has been studied, and the results are listed in Table III. The results show that the values of the coefficients are very consistent. Thus, the values of the coefficients are independent of load condition. However, there are some minor variations, which are due to anthropometric measurements.

3) Influence of Fatigue: In the context of establishment of the direct correlation between the muscular activity (during EJA change) and electrical signal (GCS data), the muscle fatigue is an important issue, which needs to be verified. Besides, fatigue is related to the decreasing the efficiency of the muscles and shows changes on electrical properties of the muscles (e.g., shift on mean frequency). Aiming to examine the influence of the fatigue on derived correlation, the muscular fatigue of the upper arm muscles has been measured during the experiment in three steps: first, second, and third minute, respectively. Certainly, the muscular fatigue can be estimated by observing the decrease of mean frequency of the EMG signal [39], [40]. Following the experimental setup in Section III-B, the muscle fatigue of the upper arm for both of the cases of the hand movements (along sagittal and transverse planes) has been displayed in Fig. 7, in which the horizontal and vertical axes refer to the time in s and mean frequency in Hz, respectively. The results show that there is muscle fatigue of the upper arm muscles during change of EJA, which are in agreement with the previous studies [41], [42]. Interestingly, the trend shows that the upper arm muscle gets fatigue faster during the forearm movement along transverse plane. However, our main objective is to study the impact of such fatigue on the calculated values of the coefficients of the polynomial functions. In this direction, the corresponding values of the polynomial coefficients for aforementioned three steps during the movement of forearm along sagittal plane

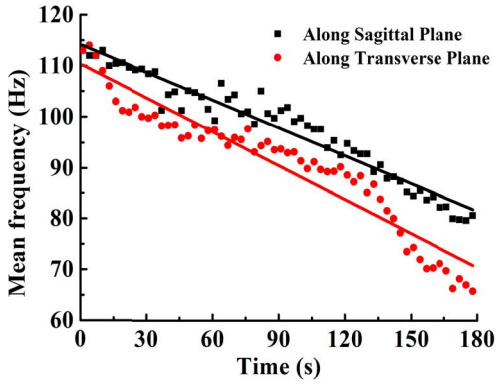

Fig. 7. Muscle fatigue during forearm movement (for 2 kg load).

TABLE IV
MEAN FREQUENCY AND POLYNOMIAL COEFFICIENTS ALONG SAGITTAL PLANE

Steps (minute)	$\theta \geq 2.3$ (linear)		$\theta < 2.3$(quadratic)		
	b_0	b_1	b_0	b_1	b_2
Load 1 kg					
First	7.1±1.1	-6.4±1.3	18.6±5.9	-33.8±13.4	15.1±7.8
Second	7.4±1.1	-6.3±1.2	19.0±6.6	-34.2±13.6	14.8±8.6
Third	7.2±0.6	-6.1±1.5	18.3±6.8	-34.1±12.8	15.4±6.3
Load 2 kg					
First	7.6±1.2	-6.8±1.1	23.6±9.1	-45.2±15.9	21.8±7.2
Second	7.8±3.1	-7.1±2.1	23.8±7.6	-46.1±13.7	22.6±7.8
Third	7.7±1.8	-7.4±2.0	24.1±7.4	-45.9±14.3	22.9±5.4

with 1 and 2 kg load are listed in Table IV. The results depict that the fatigue has very negligible effect on the coefficients.

4) Statistical Analysis: The statistical analysis has been conducted to examine the reliability of the derived correlation by considering the uncertainty factors during data acquisition followed by the impact of loads on hand and fatigue on the calculated coefficients of the polynomial. The uncertainties of the system are mainly originated from the motion tracking system (i.e., constrains of camera frame rate, precision of marker localization), signal acquisition system (i.e., quantization noise of ADC), and precise position of the electrodes.

From motion tracking system, due to constraint of the camera (capturing speed) employed in our system, which leads the error as much as 0.05 rad (2.8°) (where camera frame rate is 24 frames/s, and the forearm movement covers the total angle of 260° in back and forth on approximately 4 s). Another major source of uncertainty arises from the precise localization of the marker (see Fig. 4). As the motion data analyzer (TRACKER) calculates the actual angle by image analysis and its performance depends on the proper detection of the marker. Nevertheless, due to the limitation of this software, the detected marker point introduces jitter within a area of 5×5 mm^2. The introduced jitter leads to a maximum angle of uncertainty around 0.03 rad (1.7°) (where the radius of arc is 2.5 mm, and distance between two markers is 7 cm). In the acquisition system, the ADC resolution is 1.2 mV (14 b with full range 10 V), the quantization noise also introduces an uncertainty around 3% (1.2/40 mV) to the normalized GCS data. Other errors, such as operator error regarding actual positioning of the electrodes on different subjects. Such possible error has been encountered by conducting the experiment repeatedly upholding the elbow joint as reference for all subjects. In addition, adhesive electrodes (for both GCS and EMG) or marker have been used to minimize the motion artifacts during forearm movements. Furthermore, due to the change of physiological process in human body, the channel gain variation within three days of measurement is around 1.1 dB (3.6 mV) [26], which leads to the normalized GCS data varying around 9% (about 3.6/40 mV). Finally, the uncertainties of the system during measurement of EJA are summarized in Table V.

TABLE V
UNCERTAINTIES DURING EJA ESTIMATIONS

System level uncertainty	*Affected parameters*	*Sources*	*Measured values*
Motion tracking system	Actual angle	Camera (frame rate)	2.8^0 (4% on actual angle)
		Jitter of marker localization	1.7^0 (2% on actual angle)
Data acquisition	Received signal	ADC resolution	1.2 mV (3% on GCS data)

Next, one-way ANOVA (with $\alpha = 0.05$) analysis has been performed to study the significant differences of the values of the polynomial coefficients after conformation of homogeneity of variances by Bartlett's test ($p > 5.1$) and distributional normality by Kolmogorov–Smirnov test ($p > 1.9$) [43]. Certainly, the study has been designed in such a way, so that the influences of loading on hand and muscle fatigue can be observed separately. For instance, during the consideration of loading, the muscle fatigue has been avoided by acquiring the data for short time (about 60 s) and the subjects are given rest about 5 min in between the changing of loads; in contrast, in case muscle fatigue the data are recorded for longer time (about 3 min) with objective of gradual development of muscle fatigue (i.e., decreasing of mean frequency, see Fig. 7), while loadings are 1 and 2 kg. In each case, the residuals (ε) are also normally distributed. The calculated p values are—loading: b_0 (0.17), b_1 (0.37) for $\theta \geq 2.3$ and b_0 (0.97), b_1 (0.92), b_2 (0.82) for $\theta < 2.3$; muscle fatigue: b_0 (0.5), b_1 (0.76) for $\theta \geq 2.3$ and b_0 (0.96), b_1 (0.99), b_2 (0.95) for $\theta < 2.3$. The results show that the loading ($p > 0.17$) and muscle fatigue ($p > 0.45$) have negligible effect on the values of the polynomial coefficients; i.e., on the derived correlation as well.

B. Measurement of EJA

Now, based on the derived correlation, the EJA has been measured by performing two kinds of test—inside and outside. The inside test considers subjects (S1, S2, and S4), whose data are used during deriving the correlation. In contrast, the outside test has been performed by considering the subjects, S9–S11 (Table I). The experimental protocol including hand movements is maintained as mentioned before. Certainly, the subjects are asked to maintain certain angles, 1.0 rad (60°), 1.7 rad (100°), and 2.6 rad (150°) along the sagittal and transverse planes and the mentioned angles are estimated

TABLE VI
EJA ESTIMATION USING (10)

Type of test	Actual angle (rad)	Measured angle (rad)	Error (rad)
Inside test	2.6	2.56–2.67	0.05 (3^0)
	1.7	1.69–1.81	0.07 (4^0)
	1.0	1.02–1.11	0.07 (4^0)
Outside test	2.6	2.56–2.67	0.05 (3^0)
	1.7	1.67–1.85	0.11 (6^0)
	1.0	0.98–1.12	0.08 (5^0)

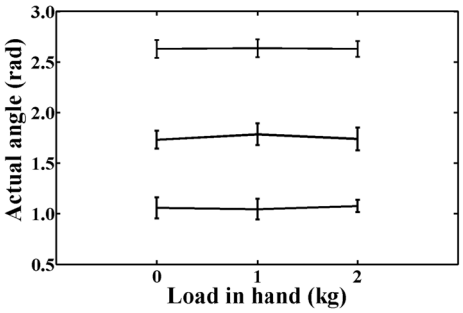

Fig. 8. Measured angles (1.0, 1.7, 2.6 rad) for different loads (empty hand, 1 and 2 kg) in hand.

based on (10) using GCS data. The measured angles are listed in Table VI. The results show that the measured angles are very consistent with maximum error of 0.11 rad (6°). As seen, the RMSEs in case of inside test are less compared with outside test. However, the overall errors are not very considerable which occurs during such anthropometric measurements very often. Moreover, one of the major advantages is that it does not involve any traditional machine-learning steps [2], [10], [11], which makes the EJA measurement very simple and easy.

The effects of load on estimated angles for outside test are plotted in Fig. 8, in which the horizontal and vertical lines are indicated the specific load and measured angle in rad respectively. The results display that the measured angles are very consistent.

C. Performance Comparison

In a performance comparison, the proposed idea has been compared with the previously proposed EJA estimation methods in the view of type of approaches, involved mechanism, system complexity, and error, which have been displayed in Table VII. The ML-based approaches encompass with very complex system configuration, and the overall system performances are dependent on the training data set, even though the consideration of diffident types of ML mechanism (e.g., ANN, BPN). Nonetheless, the complexity of the model-based approaches is moderate; however, the system performance (error) is comparatively higher. This is because of appropriate consideration of model parameters which are always being very challenging in case of modeling human activity. On the other hand, the system complexity of optimization based approaches are moderate, but the measured results are fully dependent on the acquired data and do not state any general principle toward the EJA measurement. In contrast, the proposed idea is very simple as it measures the EJA directly without involving any intermediate steps and the error is significantly low. In addition, it states a mathematical correlation between the acquired electrical data from the human muscles and change of EJA. In short, the proposed EJA measurement method is very explicit and superior to the earlier works.

TABLE VII
COMPARISONS OF THE PERFORMANCE EVALUATION

Works	Approach	Involved mechanism	System complexity	Error (rad)
[17]	Optimization	POP	Moderate	0.24 (14^0)
[4]	ML	BPN	Complex	0.20 (12^0)
[3]	ML	ANN	Complex	0.17 (10^0)
[14]	Model	Modeling	Moderate	0.31 (18^0)
[13]	ML	ANN	Complex	0.19 (11^0)
Proposed	**Direct**	**Correlation**	**Simple**	**0.11 (6^0)**

Note: POP: polynomial optimization, ANN: artificial neural network, BPN: back-propagation neural network; ML: machine learning.

V. CONCLUSION

This work proposes a simple method to measure the EJA using galvanic coupling system. First, a correlation between the changes of EJA with GCS data has been defined by a polynomial function which includes different unknown coefficients based on six-impedance model of human upper arm. Then, the values of the coefficients are determined based on the polynomial fitting technique where the actual angles are captured and calculated using motion data by a camera. Certainly, the change of EJA has been achieved by moving the forearm along the sagittal and transverse planes with different loads (empty hand, 1 and 2 kg). Next, based on the derived correlation, the EJA has been measured. In total, eleven subjects (seven males and four females) with age 30 ± 6 years have participated during the experiment. Exclusively, the GCS data of eight subjects are used to establish the correlation. The derived correlation indicates that acquired GCS data are linear at $\theta \geq 2.3$ rad, but quadric when $\theta < 2.3$ rad. Moreover, the influence of fatigue and different load on derived correlation has also been studied. The results show that muscle fatigue has very negligible influence and variation of load has no impact. The EJA has been measured in two parts—inside and outside tests. The results show that the proposed idea can measure the EJA very effectively with $\pm$ 0.11 rad (6°) of error, which is very trivial during anthropometric measurements. The proposed method of EJA measurement is very simple and easy as it does not involve any complex mechanism, such as machine learning and critical models of human arm movements. Moreover, in the performance comparison, the proposed idea demonstrates its effectiveness by showing low system complexity, higher accuracy, and easy to measure. In brief, it is a very simple and direct method for EJA measurement and is very superior compared to earlier works.

REFERENCES

[1] H.-S. Park, Q. Peng, and L.-Q. Zhang, "A portable telerehabilitation system for remote evaluations of impaired elbows in neurological disorders," *IEEE Trans. Neural Syst. Rehabil. Eng.*, vol. 16, no. 3, pp. 245–254, Jun. 2008.

[2] J. Hashemi, E. Morin, P. Mousavi, and K. Hashtrudi-Zaad, "Enhanced dynamic EMG-force estimation through calibration and PCI modeling," *IEEE Trans. Neural Syst. Rehabil. Eng.*, vol. 23, no. 1, pp. 41–50, Jan. 2015.

[3] A. T. C. Au and R. F. Kirsch, "EMG-based prediction of shoulder and elbow kinematics in able-bodied and spinal cord injured individuals," *IEEE Trans. Rehabil. Eng.*, vol. 8, no. 4, pp. 471–480, Dec. 2000.

[4] Z. H. Tang, K. Zhang, S. Sun, Z. Gao, L. Zhang, and Z. Yang, "An upper-limb power-assist exoskeleton using proportional myoelectric control," *Sensors*, vol. 14, no. 4, pp. 6677–6694, Apr. 2014.

[5] Q. Zhang, C. Zheng, and C. Xiong, "EMG-based estimation of shoulder and elbow joint angles for intuitive myoelectric control," in *Proc. IEEE Int. Conf. Cyber Technol. Autom., Control, Intell. Syst. (CYBER)*, Shenyang, China, Jun. 2015, pp. 1912–1916.

[6] R. A. R. C. Gopura, D. S. V. Bandara, J. M. P. Gunasekara, and T. S. S. Jayawardane, "Recent trends in EMG-based control methods for assistive robots," *Electrodiagnosis Frontier Clin. Res.*, vol. 1, pp. 237–268, May 2013.

[7] A. Akhtar, L. J. Hargrove, and T. Bretl, "Prediction of distal arm joint angles from EMG and shoulder orientation for prosthesis control," in *Proc. IEEE Annu. Int. Conf. Eng. Med. Biol. Soc. (EMBC)*, San Diego, CA, USA, Aug. 2012, pp. 4160–4163.

[8] M. R. Al-Mulla, F. Sepulveda, and M. Suoud, "Optimal elbow angle for MMG signal classification of biceps brachii during dynamic fatiguing contraction," in *Bioinformatics and Biomedical Engineering*. Granada, Spain: Springer, Apr. 2015, pp. 303–314.

[9] R. Tao, S. Xie, Y. Zhang, and J. W. L. Pau, "Review of EMG-based neuromuscular interfaces for rehabilitation: Elbow joint as an example," *Int. J. Biomech. Biomed. Robot.*, vol. 2, nos. 2–4, pp. 184–194, 2013.

[10] M. H. Jali, M. F. Sulaima, T. A. Izzuddin, W. Daud, W. M. Bukhari, and M. F. Baharom, "Comparative study of EMG based joint torque estimation ANN models for arm rehabilitation device," *Int. J. Appl. Eng. Res.*, vol. 9, no. 10, pp. 1289–1301, Mar. 2014.

[11] R. Raj and K. S. Sivanandan, "Estimation of elbow joint angle from time domain features of SEMG signals using fuzzy logic for prosthtic control," *Int. J. Current Eng. Technol.*, vol. 5, no. 3, pp. 2078–2081, Jun. 2015.

[12] Z. Xiao, Z. Li, and M. Chen, "Position/force estimation using hill muscle model incorporating AdaBoost with SVM-based component classifiers," in *Proc. World Congr. Intell. Control Autom. (WCICA)*, Shenyang, China, Jun. 2014, pp. 1923–1928.

[13] C. L. Pulliam, J. M. Lambrecht, and R. F. Kirsch, "EMG-based neural network control of transhumeral prostheses," *J. Rehabil. Res. Dev.*, vol. 48, no. 6, pp. 739–754, Feb. 2011.

[14] T. K. K. Koo and A. F. T. Mak, "Feasibility of using EMG driven neuromusculoskeletal model for prediction of dynamic movement of the elbow," *J. Electromyogr. Kinesiol.*, vol. 15, no. 1, pp. 12–26, Feb. 2005.

[15] Z.-Q. Zhang and J.-K. Wu, "A novel hierarchical information fusion method for three-dimensional upper limb motion estimation," *IEEE Trans. Instrum. Meas.*, vol. 60, no. 11, pp. 3709–3719, Apr. 2011.

[16] Y. Koyama, M. Nishiyama, and K. Watanabe, "A motion monitor using hetero-core optical fiber sensors sewed in sportswear to trace trunk motion," *IEEE Trans. Instrum. Meas.*, vol. 62, no. 4, pp. 828–836, Apr. 2013.

[17] H.-J. Yu, A. Y. Lee, and Y.-Choi, "Human elbow joint angle estimation using electromyogram signal processing," *IET Signal Process.*, vol. 5, no. 8, pp. 767–775, Dec. 2011.

[18] H. Zhou and H. Hu, "Reducing drifts in the inertial measurements of wrist and elbow positions," *IEEE Trans. Instrum. Meas.*, vol. 59, no. 3, pp. 575–585, Mar. 2010.

[19] A. B. B. Coutinho, B. Jotta, T. S. Carvalho, A. V. Pino, and M. N. Souza, "An alternative electrical impedance myography technique for assessment of local muscular fatigue," in *Proc. 2nd Latin Amer. Conf. Bioimpedance*, Montevideo, Uruguay, Oct. 2015, pp. 24–27.

[20] D. G. Behm, T. Cavanaugh, P. Quigley, J. C. Reid, P. S. M. Nardi, and P. H. Marchetti, "Acute bouts of upper and lower body static and dynamic stretching increase non-local joint range of motion," *Eur. J. Appl. Physiol.*, vol. 116, no. 1, pp. 241–249, Jan. 2016.

[21] G. Vescio, J. Rosell, L. Nescolarde, and G. Giovinazzo, "Muscle fatigue monitoring using a multifrequency bioimpedance technique," in *Proc. Eur. Conf. Int. Fed. Med. Biol. Eng.*, Budapest, Hungary, Sep. 2011, pp. 1257–1260.

[22] Y. Chen, X. Zhao, and J. Han, "Hierarchical projection regression for online estimation of elbow joint angle using EMG signals," *Neural Comput. Appl.*, vol. 23, no. 3, pp. 1129–1138, Jul. 2013.

[23] W. D. I. G. Dasanayake, R. A. R. C. Gopura, V. P. C. Dassanayake, and G. K. I. Mann, "Surface EMG signals based elbow joint torque prediction," in *Proc. IEEE Int. Conf. Ind. Inf. Syst. (ICIIS)*, Peradeniya, Sri Lanka, Dec. 2013, pp. 110–115.

[24] C. J. Feng and A. F. T. Mak, "Three-dimensional motion analysis of the voluntary elbow movement in subjects with spasticity," *IEEE Trans. Rehabil. Eng.*, vol. 5, no. 3, pp. 253–262, Sep. 1997.

[25] Y. Qi, C. B. Soh, E. Gunawan, K.-S. Low, and A. Maskooki, "A novel approach to joint flexion/extension angles measurement based on wearable UWB radios," *IEEE J. Biomed. Health Informat.*, vol. 18, no. 1, pp. 300–308, Jan. 2014.

[26] X. M. Chen, S. H. Pun, J. F. Zhao, P. U. Mak, B. D. Liang, and M. I. Vai, "Effects of human limb gestures on galvanic coupling intra-body communication for advanced healthcare system," *Biomed. Eng. OnLine*, vol. 15, p. 60, May 2016.

[27] Y. Song, Q. Hao, K. Zhang, M. Wang, Y. Chu, and B. Kang, "The simulation method of the galvanic coupling intrabody communication with different signal transmission paths," *IEEE Trans. Instrum. Meas.*, vol. 60, no. 4, pp. 1257–1266, Mar. 2011.

[28] M. M. Lowery, N. S. Stoykov, J. P. A. Dewald, and T. A. Kuiken, "Volume conduction in an anatomically based surface EMG model," *IEEE Trans. Biomed. Eng.*, vol. 51, no. 12, pp. 2138–2147, Dec. 2004.

[29] S. H. Pun, Y. M. Gao, P. Mak, M. I. Vai, and M. Du, "Quasi-static modeling of human limb for intra-body communications with experiments," *IEEE Trans. Inf. Technol. Biomed.*, vol. 15, no. 6, pp. 870–876, Jun. 2011.

[30] M. S. Wegmueller, M. Oberle, N. Felber, N. Kuster, and W. Fichtner, "Signal transmission by galvanic coupling through the human body," *IEEE Trans. Instrum. Meas.*, vol. 59, no. 4, pp. 963–969, Mar. 2010.

[31] F. Rabbi and K. Mohammad, "Assessment of electrode configurations of electrical impedance myography for the evaluation of neuromuscular diseases," M.S. thesis, Dept. Mech. Eng., Georgia Southern Univ., Statesboro, GA, USA, 2015.

[32] S. Baidya, K. M. Rabbi, S. Bhattacharya, and M. A. Ahad, "Identifying least affected parameters in analyzing electrical impedance myography with alteration in subcutaneous fat thickness via finite element model," in *Proc. IEEE SoutheastCon*, Fort Lauderdale, FL, USA, Apr. 2015, pp. 1–3.

[33] M. Jafarpoor, J. Li, J. K. White, and S. B. Rutkove, "Optimizing electrode configuration for electrical impedance measurements of muscle via the finite element method," *IEEE Trans. Biomed. Eng.*, vol. 60, no. 5, pp. 1446–1452, May 2013.

[34] K. M. F. Rabbi, A. Rahman, and M. A. Ahad, "Analysis of bone placements and effects of skin-fat thickness of obese in the measurement of electrical impedance myography (EIM) through finite element analysis," in *Proc. IEEE SoutheastCon*, Lexington, KY, USA, Mar. 2014, pp. 1–4.

[35] S. Gabriel, R. W. Lau, and C. Gabriel, "The dielectric properties of biological tissues: III. Parametric models for the dielectric spectrum of tissues," *Phys. Med. Biol.*, vol. 41, no. 11, pp. 2271–2293, 1996.

[36] M. A. Callejon, D. Naranjo-Hernandez, J. Reina-Tosina, and L. M. Roa, "A comprehensive study into intrabody communication measurements," *IEEE Trans. Instrum. Meas.*, vol. 62, no. 9, pp. 2446–2455, Sep. 2013.

[37] A. Cohen, "Biomedical signals: Origin and dynamic characteristics: Frequency-domain analysis," in *The Biomedical Engineering Handbook*, vol. 2. Boca Raton, FL, USA: CRC Press, 2000.

[38] Bruce C. Towe, "Bioelectricity and its measurement," in *Bioelectricity (Part 4)*. Boca Raton, FL, USA: CRC Press, 2004, ch. 17.

[39] P. Bonato, S. H. Roy, M. Knaflitz, and C. J. de Luca, "Time-frequency parameters of the surface myoelectric signal for assessing muscle fatigue during cyclic dynamic contractions," *IEEE Trans. Biomed. Eng.*, vol. 48, no. 7, pp. 745–753, Aug. 2002.

[40] S. Karlsson and B. Gerdle, "Mean frequency and signal amplitude of the surface EMG of the quadriceps muscles increase with increasing torque—A study using the continuous wavelet transform," *J. Electromyogr. Kinesiol.*, vol. 11, no. 2, pp. 131–140, Apr. 2001.

[41] T. J. Allen, M. Leung, and U. Proske, "The effect of fatigue from exercise on human limb position sense," *J. Physiol.*, vol. 588, no. 8, pp. 1369–1377, Apr. 2010.

[42] Q. Zhou, Y. H. Chen, C. Ma, and X. H. Zheng, "Evaluation of upper limb muscle fatigue based on surface electromyography," *Sci. China Life Sci.*, vol. 54, no. 10, pp. 939–944, Oct. 2011.

[43] P. Diggle, P. Heagerty, K.-Y. Liang, and S. Zeger, *Analysis of Longitudinal Data* (Oxford Statistical Science Series). Oxford, U.K.: Oxford Univ. Press, 2002.

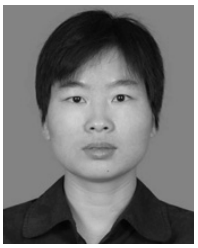

Xi Mei Chen received the master's degree with the Faculty of Science and Technology, Macau University of Science and Technology, Macau, China, in 2010, where she is currently pursuing the Ph.D. degree in electrical and computer engineering.

Her current research interests include the human body communication, body area network, and signal processing.

Shovan Barma (M'15) received the master's degree in very large scale integration (VLSI) design from Bengal Engineering and Science University, Howrah, India, in 2008, and the Ph.D. degree in electrical engineering from National Cheng Kung University, Tainan, Taiwan, in 2015.

He is currently an Assistant Professor with the Indian Institute of Information Technology, Guwahati, India. His current research interests include biomedical signal processing, affective computing, and VLSI design.

Sio Hang Pun (S'11–A'12–M'12) received the master's degree from the University of Porto, Porto, Portugal, in 1999, and the Ph.D. degree in electrical and electronics engineering from the University of Macau, Macau, China, in 2012.

He is currently an Assistant Professor with the State Key Laboratory of Analog and Mixed-Signal VLSI, University of Macau. His current research interests include biomedical electronic circuits, miniaturized sensors for biomedical applications, and human body communication.

Mang I Vai (M'92–SM'06) received the Ph.D. degree in electrical and electronics engineering from the University of Macau, Macau, China, in 2002.

He has been involved in research in the areas of digital signal processing and embedded systems since 1984. He is currently the Coordinator of the State Key Laboratory of Analog and Mixed-Signal VLSI and an Associate Professor of Electrical and Computer Engineering with the Faculty of Science and Technology, University of Macau.

Peng Un Mak (S'88–M'97–SM'11) received the B.Sc. degree in electrical engineering from National Taiwan University, Taipei, Taiwan, and the M.Sc. and Ph.D. degrees in electrical engineering from Michigan State University, East Lansing, MI, USA.

He has been the first Assistant Professor with the Department of Electrical and Computer Engineering, University of Macau, Macau, China, since 1997. He has authored or co-authored over 140 peer-reviewed technical publications (journal, book chapter, and conference proceedings). His current research interests include biosignals extraction and processing, bioelectromagnetism, human body communication, and body sensor network.

Dr. Mak is a member of Phi Kappa Phi and Eta Kappa Nu (currently IEEE-HKN).